Estimating Remaining Lifetime of Electrical Insulations in motor windings Based on Measured Indicators

Nesrine DJEDDOU[1, 2], Stéphane DUCHESNE[1], Fabrice MORGANTI[1], Olivier DEBLECKER[2], Bashir BAKHSHIDEH ZAD[2].

[1] Univ. Artois, UR 4025, Laboratoire Systèmes Électrotechniques et Environnement (LSEE), Béthune, F-62400, France.

[2] EPEU Unit, Polytech of Mons, 7000 Mons, Belgium.

ABSTRACT - The lifetime of electrical machines is closely related to the degradation of stator winding insulation. Non-destructive diagnostic techniques, such as capacitance measurements and partial discharge (PD) analysis, are widely used to monitor this degradation. This study proposes a methodology to predict the remaining lifetime of electrical insulation systems based on measured indicators. Using artificial intelligence (AI) tools, four predictive models were developed to estimate insulation lifetime from the evolution of the Partial Discharge Inception Voltage (PDIV) over time. The best performance was achieved using an Artificial Neural Network (ANN), with an R^2 value of 0.983. Additionally, this work enables the separate investigation of electrical and thermal aging processes. It also explores how the two indicators PDIV and parallel capacitance (Cp) provide an insight into different aging mechanisms.

Keywords — Electrical insulation, AI, Aging, Indicator, Lifetime.

1. INTRODUCTION

Rotating electrical machines are particularly susceptible to insulation degradation, a gradual aging process that can span several years. This phenomenon, which affects the lifespan of equipment, represents a significant challenge for engineers and industrial maintenance managers. Two important studies highlight the extent of this phenomenon. The first, conducted by General Electric, analyzed 5000 three-phase squirrel-cage motors from various industrial sectors. It revealed that 37% of failures involved stators, 11% of which were specifically related to insulation systems [1]. The second study, conducted by CIGRE, shows that 56% of hydrogenerator failures are due to defects in insulation systems [2]. Finally, a complementary study on 1199 devices identifies three main causes of insulation system failure: insulation aging (responsible for 31% of problems), the occurrence of partial discharges (22%), and contamination or pollution (25%) [3].

The aging of insulation systems begins with the deterioration of the coil insulation, which then spreads to the insulation between phases or between phase and ground, leading to a progressive decrease in coil resistance [4]. This process is particularly concerning because it can lead to unforeseen mechanical and electrical failures. As insulating materials age, they become more sensitive to the various stresses they are subjected to. These factors are referred to as TEAM stresses (Thermal, Electrical, Ambient, and Mechanical). Thermal stress is due to the operating temperature, caused by Joule losses, eddy current losses, and hysteresis losses, and it is considered the dominant factor in long-term aging. Electrical stress has been addressed in several studies, especially in medium-voltage machines, where partial discharges occur as a result of the high voltage gradients (dv/dt) imposed by the inverter supply, and is further influenced by the the use of new power semiconductors devices based on SiC or GaN technology. Ambient stress refers to environmental factors such as humidity and radiation effects. Mechanical stress is caused by the movement of the coils and the magnetic forces generated by the current flow. All these stresses directly influence the lifespan of the stator and rotor winding insulation systems [5], progressively degrading the insulation integrity until its dielectric strength is compromised, eventually leading to insulation failure, which can be either permanent or temporary [6-8].

In this context, it is essential to better understand the underlying mechanisms of insulation aging and predict their behavior over time to extend the lifespan of machines and avoid costly failures. This work aims to use artificial intelligence to model these phenomena and predict the remaining life of insulations. The adopted approach relies on the collection of electrical data, such as parallel resistance (Rp), parallel capacitance (Cp), partial discharge inception voltage (PDIV), and dissipation factor (D) as aging indicators, as demonstrated in previous studies [9-11]. These measured data are then used to train selected artificial intelligence algorithms to estimate the condition of insulation systems. By leveraging experimental data from an aging indicator that reflects the state of the coil insulation, the predictive model estimates the remaining life of the insulation while accounting for the various factors influencing its degradation influencing its degradation.

The remainder of this paper is organized as follows. Section 2 reviews the literature on empirical and AI-based models for assessing the aging of electrical insulation systems. Section 3 describes the experimental setup, including the twisted pair specimens and the accelerated aging procedure. Section 4 presents the aging indicators measured during the experiments and their evolution over time. Section 5 details the development of aging prediction models using both linear regression and AI techniques. Finally, Section 6 summarizes the main findings and outlines directions for future research.

2. LITERATURE REVIEW

Studies have been conducted using in each case a single indicator to optimize time, and comparing the results with other conventional methods. [12-14].

2.1. *Insulation Resistance for Lifetime Optimization*

Insulation resistance is one of the most commonly used parameters to assess the condition of insulation systems in electric motors. It typically decreases with increasing temperature, electrical stresses, and charge/discharge cycles. Studies [12][13] have shown that by monitoring insulation resistance, it is possible to predict the long-term lifespan under thermal aging at different temperatures. Several curve fitting models and Bayesian Regularization Backpropagation BRP neural network neural network have been employed. BRP relies on a feedforward architecture and adjusts weights and biases through iterative forward and backward passes to minimize prediction errors, while Bayesian regularization helps prevent overfitting and improves generalization. The results obtained from these models were used to generate Arrhenius plots, linking temperature to insulation lifespan. However, despite these modeling efforts, the accuracy of aging time predictions remains limited.

2.2. *Insulation Capacitance for Lifetime Optimization*

Insulation capacitance is an important indicator for assessing the condition of insulation. A study conducted on motorettes [14], subjected to thermal stresses at different temperatures, showed that this capacitance can be used to track the evolution of insulation over time. Measurements are taken at each cycle and used to establish an empirical equation that links time to the behavior of insulation capacitance. This allows for predicting the evolution of insulation over the course of thermal cycles.

Additionally, research at the LSEE laboratory has shown that Cp [9] [15] is a promising indicator for assessing insulation aging. This indicator is now integrated into machine monitoring systems, as illustrated in Fig. 1, to monitor the purely thermal aging of a standard wire, where a progressive increase in ΔC is observed over time. Concurrently, it was observed that PDIV decreases as the organic layers age.

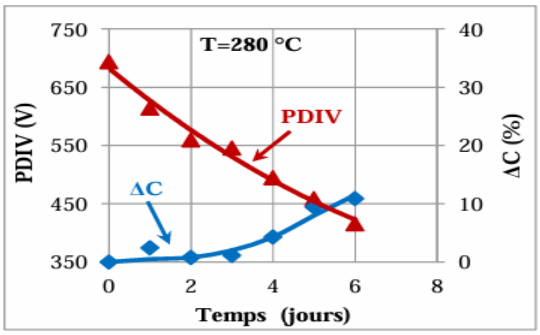

Fig. 1: Variation of Capacitance and PDIV as a Function of Aging Duration for 1-Day Cycles at 280°C [9].

3. Proposed Experimental Methodology

Before proceeding with the studied samples, our experimental approach focused on taking measurements of two indicators, PDIV and Cp. The procedure will be described in the upcoming subsection.

3.1. *Studied samples*

Standardized twisted specimens were prepared using wire with a diameter of 1.25 mm, rated for a thermal class of 210°C, and coated with a double layer of insulation : polyamide-imide (PAI) and polyesterimide (PEI). Each specimen was 200 mm long, consisting of six turns, and subjected to a tension force of 7 N. These specimens were prepared in accordance with IEC 270 [16'] using a standardized TURNS device from RIGON.

3.2. *Measured Characteristics*

Measurements of Cp were performed using the Agilent 4980A Precision LCR Meter at a frequency of 10 kHz. According to the measurement methods defined by IEC 62631-1 [66], the measurement frequency was selected based on the instrument's accuracy specification in the datasheet (10 kHz – 0.005% precision).

PDIV measurements were carried out inside a Faraday cage in accordance with IEC 60270 [18]. For each specimen, 11 tests were performed to calculate the mean PDIV value. All measurements were conducted at ambient temperature. The measurement setup, shown in the electrical diagram in (Fig. 2), includes a 1nF coupling capacitor for partial discharge and voltage measurement, with signals amplified by a preamplifier (RPAI). All components were placed inside a Faraday cage to eliminate electromagnetic interference. The ICM Compact displays partial discharge pulses on a sinusoidal voltage signal, identifying the PDIV when repetitive pulses begin to appear.

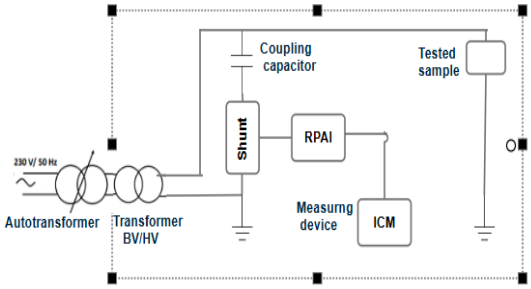

Fig. 2: The electrical diagram of the Faraday cage.

3.3. *Thermal and Electrical Aging Procedures*

The samples were subjected to controlled electrical aging conditions using the electrical aging setup shown in (Fig. 3). This setup includes a function generator (GBF) connected to two amplifiers that amplify the signal to deliver the required voltage levels. A Raspberry Pi is used to collect and store data from the system. The setup also features a test box containing two samples, along with an interface designed to monitor and record their lifespan under the applied electrical stresses.

Two electrical stress levels were applied: 850 V (1.3 × PDIV) with 24-hour cycling, and 1000 V (1.5 × PDIV) with 16-hour cycling. In both cases, a sinusoidal voltage at a frequency of 1 kHz was used.

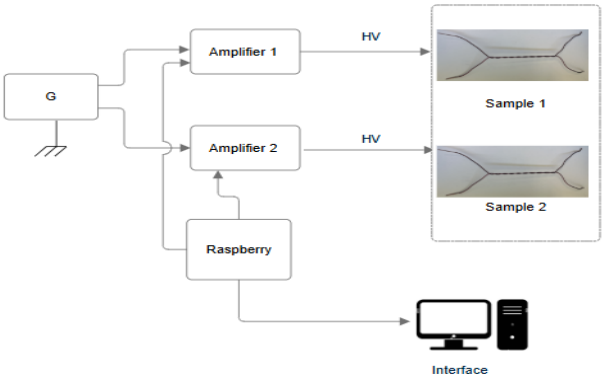

Fig. 4: Electrical aging setup.

In addition to the electrical aging tests, a thermal aging process was carried out using a high-temperature oven at 290 °C, applying a 5-hour cycle to five test specimens. This initial single-temperature test was conducted solely to observe the evolution of the indicators over time and to compare their behavior with that observed under electrical aging.

4. Results and Discussions

4.1. Analysis of Indicators

The electrical analysis of Cp and PDIV indicators, along with temperature measurements taken by thermocouple starting from 144 hours (Fig. 4) reveals that under a relatively stable temperature and an applied voltage of 850 V (approximately 1.3 times the initial PDIV), Cp tends to increase following the trend line. This increase may be explained by the fact that partial discharges can locally modify the insulating layers, creating regions of high permittivity. Additionally, the thickness of the insulation tends to decrease with electrical aging, which could also contribute to the increase in capacitance.

Regarding the PDIV, it exhibits a relatively stable trend throughout the aging process, as shown by the trend line. This indicates that few partial discharges were initiated during the test, suggesting that the effect of electrical aging alone is not very pronounced in this case. As a result, the PDIV remains nearly constant over time, which makes it difficult to use directly as a reliable degradation indicator.

Therefore, further research is needed to better understand how the material properties evolve under electrical stress, how environmental conditions may influence this evolution, and whether the effect is purely electrical or enhanced by higher voltage levels. As observed in (Fig. 5), increasing the applied voltage results in higher PDIV values, indicating that this approach could offer more potential for studying electrical aging phenomena.

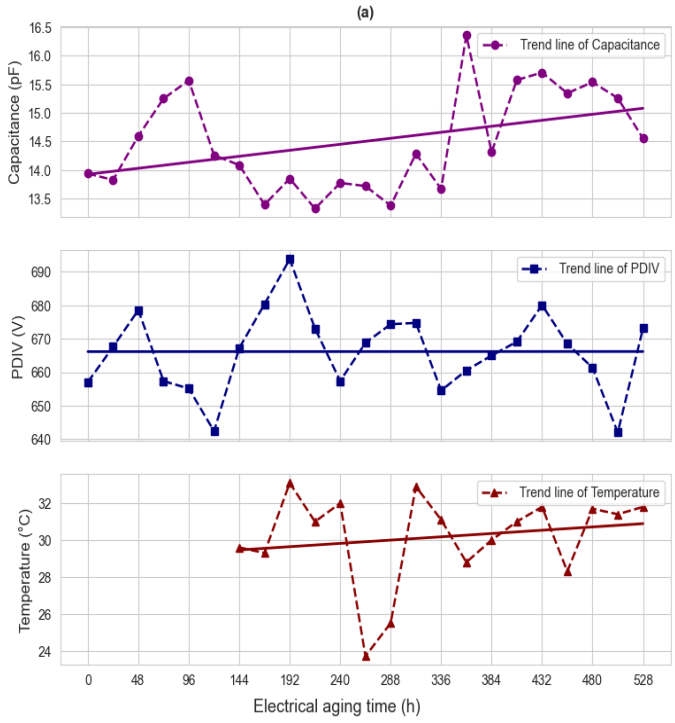

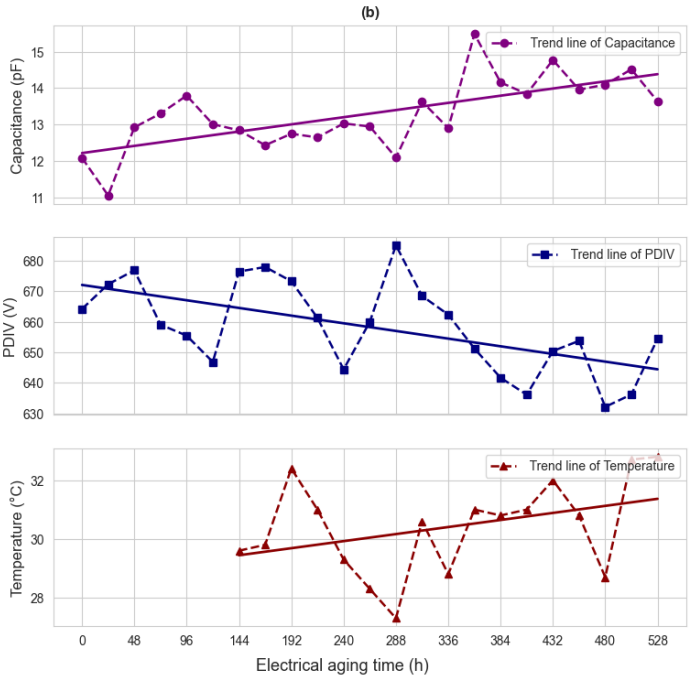

Fig. 4: Experimental Results of Indicators at 850 V Electrical Aging: (a) Specimen 1, (b) Specimen 2.

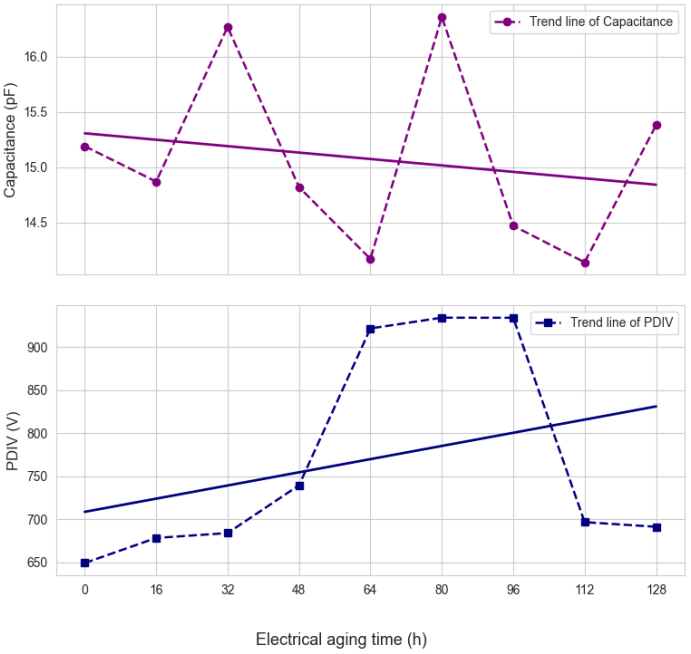

Fig. 5: Experimental Results of Indicators at 1000 V Electrical Aging: Specimen 1.

Previous studies [9,15] have demonstrated that PDIV tends to decrease during thermal aging due to the progressive degradation of insulation. This behavior is also confirmed by our experimental results (Fig. 6), which show a clear decline in PDIV over time. The decrease is mainly caused by the thinning of the insulation and the emergence of defects both on the surface and within the material. These imperfections create localized areas of high electric field, which promote dielectric breakdown [6].

Meanwhile, Cp typically increases during the initial stages of aging. This is followed by what is known as the avalanche effect: as partial discharges occur, capacitors initially store charge but begin to release it as the energy builds up, leading to a gradual decrease in Cp over time [19].

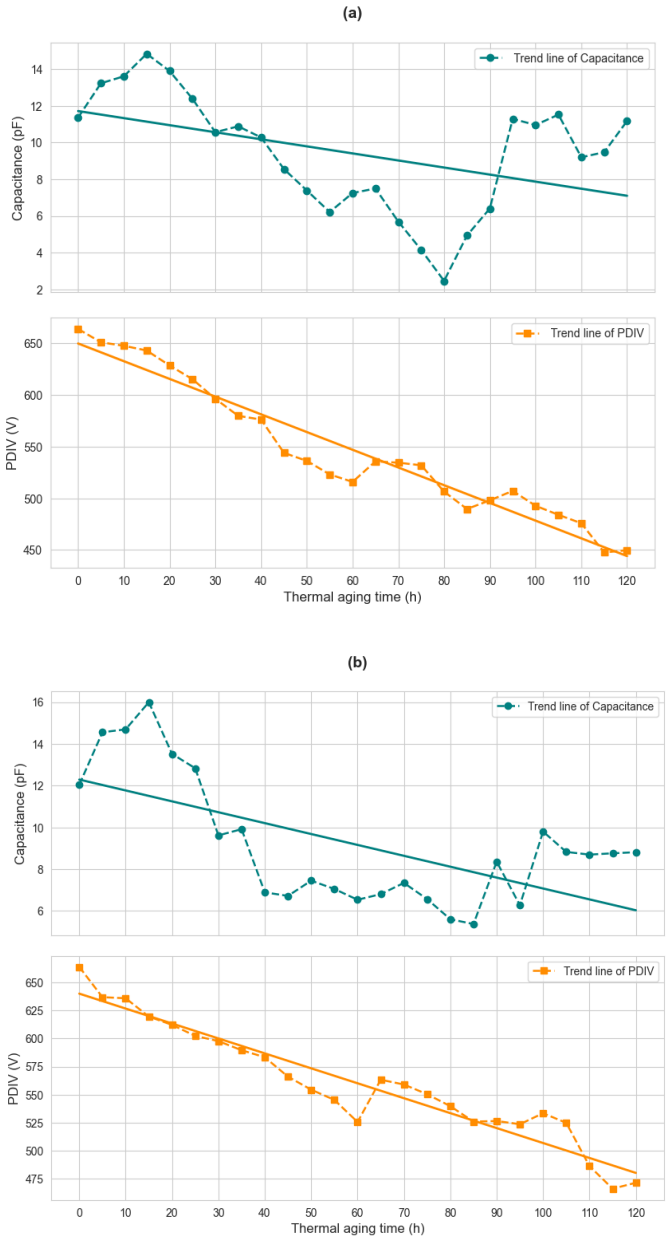

Fig. 6: Experimental Results of Indicators under Thermal Aging at 290°C: (a) Specimen 1, (b) Specimen 2.

5. AI Model Results for Lifetime Prediction of Insulation Based on PDIV Measurements

In this article, four models are used to predict the lifetime of the specimens based on a single aging indicator, namely the PDIV. Among these models, one is based on an Artificial Neural Network (ANN) using a multilayer perceptron (MLP) similar to the approach described in [20].

This MLP model is designed to learn the relationship between thermal aging time and the remaining lifetime of electrical insulation systems. It consists of six hidden layers, each containing 512 neurons, and uses the ReLU activation function to introduce non-linearity. Optimization is performed using the Adam algorithm, which applies backpropagation to minimize prediction error.

To evaluate the model, the Leave-One-Out Cross-Validation (LOOCV) method is applied, particularly well-suited for small datasets (here, only five data samples). In each iteration, four specimens are used for training and one for testing, rotating the test specimen each time.

The model follows the typical MLP x architecture equations:

$$z_j = \sum_{i=1}^{n} W_{ji} x_i + b_j \quad (1)$$

$$a_j = f(z_j) \quad (2)$$

$$\hat{y} = f_{out} \sum_{j=1}^{m} W_{jk} a_j + b_K \quad (3)$$

- x_i: Input features for training (in our case, aging time t_i).
- W_{ji}: Weights learned by the MLPRegressor during training on x_train and y_train.
- b_j: Bias associated with hidden neuron j.
- z_j Pre-activation output calculated using equation (1).
- a_j: Activated output of hidden neuron after applying the activation function, (equation (2)); corresponding here to the PDIV value.
- W_{jk}: Weights connecting hidden neuron j to the output layer.
- b_K: Bias of the output layer.
- f_{out}: Activation function used at the output layer.
- $\widehat{y_i}$: Final predicted value of the model.

In addition to the ANN, three other models were applied to predict the evolution of PDIV over time, in order to estimate the aging of the insulation system under thermal stress. First, polynomial regression was used, which fits a non-linear polynomial relationship between time and the PDIV indicator. This allows capturing more complex trends beyond simple linear regression. Additionally, two machine learning models were employed:

- Support Vector Regression (SVR), which is an adaptation of Support Vector Machines for regression problems. SVR works by finding a function that deviates from the actual observed values by no more than a specified margin (ε), while ensuring the function is as flat as possible.

- K-Nearest Neighbors (KNN), which predicts the value at a given time by averaging the outputs of the k most similar (nearest) data points in the training set.

Both SVR and KNN were inspired by methods previously used for battery lifetime prediction [21][22] and have been widely applied to various regression tasks. In this work, they were adapted to predict the degradation of insulation systems.

Once the PDIV predictions over time are obtained, the remaining lifetime is estimated by defining a critical threshold 450, which was determined through a hipot test applying 1000 V to the specimen. This test showed that the specimen cannot withstand this voltage, and all specimens failed at a PDIV value

of approximately 450 V. The series of predicted values is examined to identify the first moment when the predicted curve drops below this threshold. The time corresponding to this crossing point is then considered the estimated remaining lifetime of the system. This method allows for evaluating, based solely on predictions, when the system will reach a critical operating limit, even without relying on other parameters such as temperature.

This corresponds to the following equation (4):

$$t_{\text{end}} = min\{t | PDIV_{\text{predicted}}(t) \leq critical\ threshold\} \quad (4)$$

- t_{end} : estimated remaining lifetime (the time when the limit is reached).
- $PDIV_{\text{predicted}}(t)$: predicted PDIV value at time t.
- critical threshold: the set threshold value (450).

Two chosen specimens were selected for prediction across the different models compared to the true (measured) values (Fig. 7, Fig. 8). We observe that the ANN predictions are highly similar to the real measured curves. Metrics were calculated to study the error between the predicted and measured values.

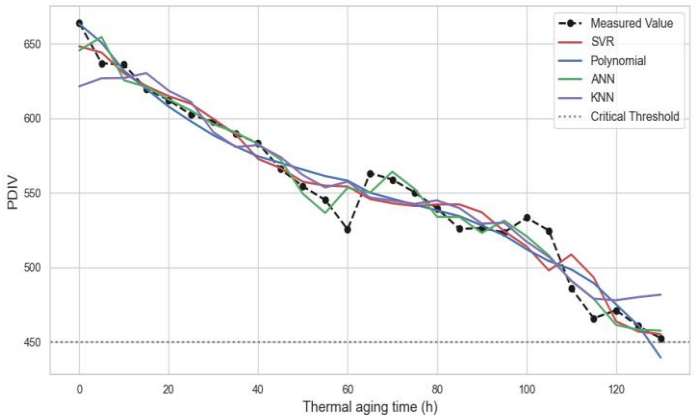

Fig. 7: Predicted Results at 290°C Thermal Aging: Specimen 1.

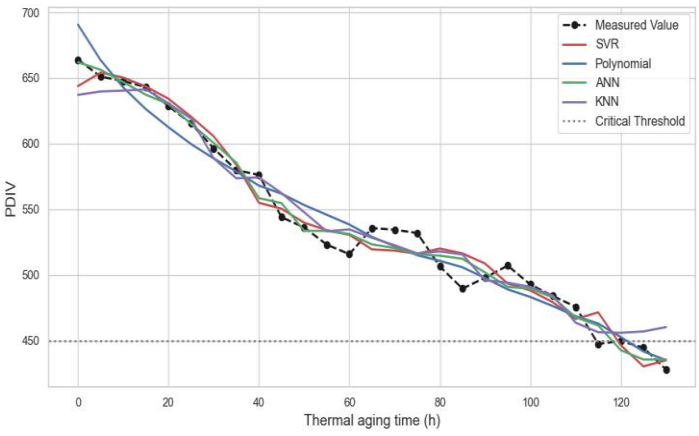

Fig. 8: Predicted Results at 290°C Thermal Aging: Specimen 2.

For evaluating model performance in this regression problem, we chose R^2 and MRE as the key metrics. These metrics are well-suited for regression tasks and are particularly effective for assessing the performance of models such as ANN, SVR, Polynomial Regression, and KNN in predicting complex systems such as the degradation of electrical insulation.

R^2 (Coefficient of Determination):

It measures the proportion of the variance in the actual data that is explained by the regression model. An R^2 value close to 1 indicates a very good model fit, while close to 0 it indicates a poor fit as shown in (5).

$$R^2 = 1 - \frac{\sum_{i=1}^{n} \left(y_{\text{true,i}} - y_{\text{pred,i}}\right)^2}{\left(y_{\text{true,i}} - \bar{y}_{\text{true}}\right)^2} \quad (5)$$

MRE (Mean Relative Error):

MRE is a metric used to assess the average of the relative errors between the predicted and actual values over a dataset. The relative error gives us an understanding of the prediction error in proportion to the true value, and MRE aggregates this over all data points to provide a summary measure of model accuracy y.

$$\text{MRE\%} = \frac{1}{n} \sum_{\mathbf{i=1}}^{\mathbf{n}} \frac{\left|y_{\text{true,i}} - y_{\text{pred,i}}\right|}{\left|y_{\text{true,i}}\right|} * 100 \quad (6)$$

- $y_{\mathbf{true,i}}$: The actual value of the i-th observation.
- $y_{\mathbf{pred,i}}$: The predicted value for the i-th observation.
- $\bar{y}_{\mathbf{true}}$: The mean of the true values.
- n: The number of data points.

The performance metrics presented in Table 1, along with the boxplot in Fig. 9, illustrate the distribution of relative errors (%) for four regression models: Support Vector Regression (SVR), Polynomial Regression, Artificial Neural Network (ANN), and K-Nearest Neighbors (KNN). Among these, the ANN model demonstrates the lowest median relative error (~0.8%) and the least variability, indicating strong stability and consistency in its predictions. In contrast, SVR and Polynomial models exhibit slightly higher median errors, while the KNN model shows a broader error distribution with several outliers, reflecting greater sensitivity to local data variations. This visual analysis is further supported by the values of R^2, which evaluate the overall predictive accuracy of each model. ANN achieves the best performance with an R^2 of 0.983, followed by SVR (0.974), Polynomial Regression (0.969) and KNN (0.955). These results clearly indicate that ANN outperforms the other models.

Description	SVR	Polynomial Regression	KNN	ANN
R^2	0,974	0.969	0.955	0.983
MRE %	1.56	1.70	2.11	1.20

Table1: Predicted Metrics for Thermal Aging at 290°C calculated overall Specimens.

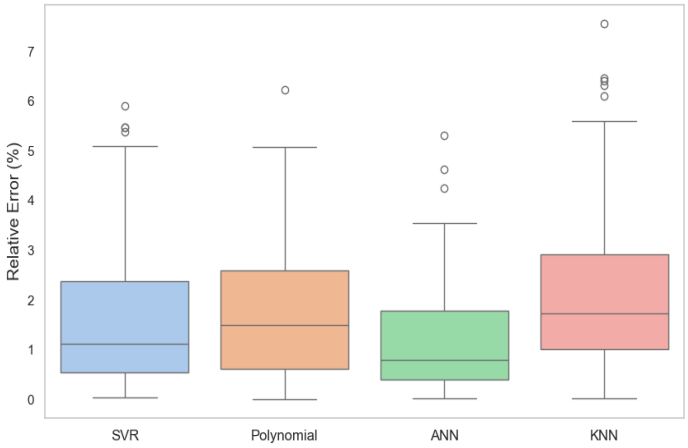

Fig. 9: Boxplot of Prediction Errors for SVR, Polynomial, ANN, and KNN.

6. Conclusions and Perspectives

Different specimens were tested separately under thermal and electrical aging to evaluate how indicators such as Cp and PDIV evolve over time. The results show that these indicators are not significantly affected under electrical aging, making them difficult to exploit and interpret. This could be due to specific physical behaviors of the insulation material, which should be investigated in future work.

In contrast, thermal aging showed more evident effects, with variations in the indicators consistent with findings from the literature. These results confirm that thermal aging can be tracked to assess the insulation condition of the machine over time. Based on this, we were able to predict the remaining useful life using a single indicator, achieving a high determination coefficient (R^2= 0.983) with ANN model at this initial stage of the study.

However, in real operating conditions, the machine is subjected to both thermal and electrical aging. It is therefore essential to identify the most relevant indicator under combined stress. In this context, we plan to focus on reflectometry, which we aim to develop and apply to partial discharge aging. This technique could help detect localized degradation and provide more accurate insights into the aging process.

Additionally, future work should involve testing the models at different temperatures to better replicate real-world operating conditions. It should also explore the interaction between thermal and electrical stresses — particularly how thermal aging may accelerate electrical degradation — in order to predict lifetime under multiple stress factors and generalize the approach to actual winding systems.

7. Acknowledgments

This research project is being conducted jointly with the University of Mons (Electrical Power Engineering Unit - EPEU). It is part of the ANR MYEL project (ANR-22-LCV2-0001 MYEL), a joint laboratory initiative involving the LSEE and LGI2A laboratories, as well as the company CRITT M2A.

8. References

[1] E. Cornell, E. Owen, J. Appiarius, R. McCoy, P. Albrecht, and D. Houghtaling, Improved motors for utility applications. Final report, Schenectady, NY, USA: General Electric Co., 1982.

[2] CIGRE Study Committee SC11, “Hydrogenerator failures–results of the survey,” 2003.

[3] R. Brütsch, M. Tari, K. Fröhlich, T. Weiers, and R. Vogelsang, “Insulation failure mechanisms of power generators,” IEEE Electr. Insul. Mag., vol. 24, no. 4, pp. 17–25, Jul. 2008.

[4] D. Barater, F. Immovilli, A. Soldati, G. Buticchi, G. Franceschini, C. Gerada, and M. Galea, “Multistress characterization of fault mechanisms in aerospace electric actuators,” IEEE Trans. Ind. Appl., vol. 53, no. 2, pp. 1106–1115, Mar./Apr. 2017.

[5] Ghassemi M. Ghassemi, “Accelerated insulation aging due to fast, repetitive voltages: A review identifying challenges and future research needs,” IEEE Trans. Dielectr. Electr. Insul., vol. 26, no. 5, pp. 1558–1568, Oct. 2019.

[6] IEEE Std 1043-1996, IEEE Recommended Practice for Voltage Endurance Testing of Form Wound Bars and Coils, IEEE, 1996.

[7] K. Sathiyasekar, K. Thyagarajah, and A. Krishnan, “Neuro-fuzzy based prediction of insulation quality of high voltage rotating machines,” Expert Syst. Appl., vol. 38, pp. 1066–1072, 2011.

[8] G. C. Stone, “Partial discharge diagnostics and electrical equipment insulation condition assessment,” IEEE Trans. Dielectr. Electr. Insul., vol. 12, no. 5, pp. 891–904, Oct. 2005.

[9] S. Savin, Nouvel indicateur de vieillissement de l'isolation inter-spires des machines électriques utilisées en aéronautique, Ph.D. dissertation, Univ. Artois, 2013.

[10] P. Pietrzak, Mise au point de méthodes d'essais et d'analyse permettant le test-multi-contraintes, le suivi du vieillissement et/ou la modélisation de durée de vie du système d'isolation employé dans les moteurs électriques utilisés dans les futures automobiles hybrides, hybrides rechargeables et tout électriques, Ph.D. dissertation, INPT Toulouse, 2023.

[11] S. Xiang, G. Li, F. Zhou, S. Huang, Z. Xu, G. Jia, and F. Niu, “Life prediction of ground-wall insulation material in electric motors based on accelerated degradation test under different failure mechanisms,” IEEE J. Emerg. Sel. Topics Ind. Electron., Dec. 2024.

[12] G. Turabee, M. R. Khowja, P. Giangrande, V. Madonna, G. Cosma, G. Vakil, C. Gerada, and M. Galea, “The role of neural networks in predicting the thermal life of electrical machines,” IEEE Access, vol. 8, pp. 40283–40297, Feb. 2020.

[13] M. R. Khowja et al., “Lifetime estimation of enameled wires under accelerated thermal aging using curve fitting methods,” IEEE Access, vol. 9, pp. 18993–19003, Jan. 2021.

[14] V. Madonna, P. Giangrande, G. Migliazza, G. Buticchi, and M. Galea, “A time-saving approach for the thermal lifetime evaluation of low-voltage electrical machines,” IEEE Trans. Ind. Electron., vol. 66, no. 11, pp. 9195–9205, Nov. 2019.

[15] G. Pereira Dos Santo Lima, S. Ait-Amar, and G. Velu, “Study of new ecological magnet wires performances during thermal aging tests,” in Proc. IEEE Int. Conf. Dielectr. (ICD), 2022.

[16] AFNOR, IEC 60270 COMPIL, Nov. 2015.

[17] ASTM D1676-03, Standard Test Methods for Film-Insulated Magnet Wire, ASTM International, West Conshohocken, PA, USA, 2011.

[18] IEC 60270, High-voltage test techniques – Partial discharge measurements, 2000.

[19] C. Garry, L’effet de couronne en tension alternative, Paris, France: Direction des Études et Recherches, EDF, 1976.

[20] G. Rigtos, P. Siano, and A. Piccolo, “Neural network-based approach for early detection of cascading events in electric power systems,” IET Gener. Transm. Distrib., vol. 3, no. 7, pp. 650–665, Jul. 2009.

[21] Y. Chen, W. Duan, Z. Ding, and Y. Li, “Battery life prediction based on a hybrid support vector regression model,” Front. Energy Res., vol. 10, article 899804, 2022.

[22] X. Sui, S. He, S. B. Vilsen, J. Meng, R. Teodorescu, and D.-I. Stroe, “A review of non-probabilistic machine learning-based state of health estimation techniques for lithium-ion battery,” Appl. Energy, vol. 300, article 117346, 2021.